ORIGINAL ARTICLE

Visual Contrast Sensitivity Improvement by Right Frontal High-Beta Activity Is Mediated by Contrast Gain Mechanisms and Influenced by Fronto-Parietal White Matter Microstructure

Romain Quentin[1], Seth Elkin Frankston[1,2], Marine Vernet[1], Monica N. Toba[1,5,6], Paolo Bartolomeo[1,3], Lorena Chanes[1], and Antoni Valero-Cabré[1,2,4]

[1]Cerebral Dynamics, Plasticity and Rehabilitation Group, Frontlab, Centre de Recherche de l'Institut du Cerveau et de la Möelle Epinière, ICM, CNRS UMR 7225, INSERM UMRS 1127 and Université Pierre et Marie Curie, Paris, France, [2]Laboratory for Cerebral Dynamics Plasticity and Rehabilitation, Boston University School of Medicine, Boston, MA, USA, [3]Department of Psychology, Catholic University, Milan, Italy, [4]Cognitive Neuroscience and Information Technology Research Program, Open University of Catalonia (UOC), Barcelona, Spain, [5]Laboratory of Functional Neurosciences (EA 4559), University Hospital of Amiens, France, and [6]University of Picardy Jules Verne, France

Address correspondence to Dr Antoni Valero-Cabré, CNRS UMR 7225,INSERM U 1127, Université Pierre et Marie Curie, ICM, Groupe de Dynamiques Cérébrales, Plasticité et Rééducation, Frontlab, Hôpital de la Salpêtrière, 47-boulevard de l'Hôpital, 75651 Paris Cedex 13, France. Email: avalerocabre@gmail.com; avalero@bu.edu

Abstract

Behavioral and electrophysiological studies in humans and non-human primates have correlated frontal high-beta activity with the orienting of endogenous attention and shown the ability of the latter function to modulate visual performance. We here combined rhythmic transcranial magnetic stimulation (TMS) and diffusion imaging to study the relation between frontal oscillatory activity and visual performance, and we associated these phenomena to a specific set of white matter pathways that in humans subtend attentional processes. High-beta rhythmic activity on the right frontal eye field (FEF) was induced with TMS and its causal effects on a contrast sensitivity function were recorded to explore its ability to improve visual detection performance across different stimulus contrast levels. Our results show that frequency-specific activity patterns engaged in the right FEF have the ability to induce a leftward shift of the psychometric function. This increase in visual performance across different levels of stimulus contrast is likely mediated by a contrast gain mechanism. Interestingly, microstructural measures of white matter connectivity suggest a strong implication of right fronto-parietal connectivity linking the FEF and the intraparietal sulcus in propagating high-beta rhythmic signals across brain networks and subtending top-down frontal influences on visual performance.

Key words: brain, fronto-parietal connectivity, non-invasive neurostimulation, oscillation, superior longitudinal fasciculus, synchronization, visual perception, visuo-spatial attention, white matter anatomy

Introduction

Local oscillations and interregional synchrony are considered as crucial processes for the understanding of cognitive coding throughout brain networks. Although the causal nature of such contributions remains to be fully demonstrated, a significant number of animal and human studies have highlighted associations between oscillation frequency and cognitive operations (Buzsáki and Draguhn 2004; Fries 2005; Cannon et al. 2014). In the human attention and perception domain, for example, alpha oscillations in occipito-parietal areas have been found highly correlated with the orienting of attention in space (Foxe et al. 1998; Worden et al. 2000; Sauseng et al. 2005) and capable to predict visual detection performance (Ergenoglu et al. 2004; Thut et al. 2006; Gould et al. 2011). At higher frequency bands, fronto-parietal synchronization at the high-beta band (22–34 Hz) has been reported to signal in both monkeys (Buschman and Miller 2007) and humans (Phillips and Takeda 2009), the deployment of endogenous spatial orienting during a visual search paradigm.

This emerging field of research has thus far relied on correlational evidence. However, the recently developed ability to entrain brain oscillatory activity with rhythmic patterns of transcranial magnetic stimulation (TMS) provides a unique non-invasive approach to enrich with causal evidence the above-mentioned associations in human participants. Indeed, non invasive stimulation methods combined with interleaved EEG recordings have substantiated evidence of oscillation phase resetting (Fuggetta et al. 2005; Van Der Werf and Paus 2006), enhancements of natural rhythms characteristic of a cortical region (Rosanova et al. 2009), and also the episodic entrainment of regional oscillatory activity at the input frequency with short bursts of rhythmic TMS (Thut et al. 2011). Furthermore, these rhythmic patterns have demonstrated the ability to modulate specific aspects of human visuo-spatial cognition, such as visual short-term memory capacity, global versus local feature-based attention, and visual sensitivity (Sauseng et al. 2009; Romei et al. 2010, 2011, 2012; Chanes et al. 2013).

In a prior study using this approach, we demonstrated that pre-target rhythmic patterns delivered to the right frontal eye field (FEF) and tuned to the high-beta range (30 Hz) enhanced visual sensitivity for near-threshold targets (Chanes et al. 2013). To isolate the specific contribution of the oscillation frequency, the impact of non-uniform bursts with an equal number of pulses delivered at the same pre-target onset time window, or the impact of gamma (50 Hz) bursts, was also tested along and compared with the former, showing no impact on visual performance. Interestingly, high-beta-specific modulations of visual sensitivity proved strongly correlated with interindividual differences in the volume of the first branch of the superior longitudinal fasciculus (SLF), linking the stimulated FEF region with the intraparietal sulcus (IPS) in the right hemisphere (Quentin et al. 2015). This finding provided novel support for the notion that white matter structure and myelination properties might strongly influence interregional synchronization at a specific frequency band (Zaehle and Herrmann 2011). However, prior evidence collected in Chanes et al. (2013) compared the effects of rhythmic frequency specific and rhythmic non-frequency specific patterns, instead of random activity of equal duration and pulse number. Additionally, results were restricted to near-threshold vision, and hence it remains to be explored whether similar frequency-specific modulatory effects hold or not for a full spectrum of stimulus contrast levels. The answer to this question is important as it could help rule out whether the modulatory effects engaged by high-beta frontal patterns are or not independent of stimulus intensity, and thus, respectively, mediated by a contrast gain or a response gain effect (Reynolds and Desimone 1999; Carrasco et al. 2004). Moreover, sensory gain processes, which have been extensively studied in visual perception using psychophysical methods, are thought to reflect attention-driven modulations of neuronal activity in striate and extrastriate visual areas (Ling and Carrasco 2006; Pestilli et al. 2007, 2009) and the presence of sensory gain-like processes could suggest additional links between the effects of right frontal rhythmic patterns on visual performance and attention-orienting mechanisms.

Hence, here we employed a complete psychometric contrast sensitivity function to determine whether the facilitatory effects on visual performance induced by *high-beta frequency-specific* right FEF activity (when compared with a *random non-frequency-specific* activity) could also be extended to other stimulus contrast levels. In this same population of participants, the anatomical connectivity estimates of white matter pathways linking frontal and parietal sites, and specifically those known to depart from the stimulated right FEF, were correlated to behavioral outcomes and employed to further support a potential role for fronto-parietal anatomical networks in propagating high-beta rhythmic signals across systems subtending the modulation of visual performance.

Materials and Methods

Study Participants

A group of 14 right-handed participants (9 women and 5 men, mean age = 24.2 ± 3.0 years) reporting no history of neurological or psychiatric disorders and a normal or corrected-to-normal vision took part in this experiment. All participants freely provided informed written consent prior to their participation and were compensated for taking part in the study. The protocol was reviewed by the INSERM (*Institut National de la Santé et de la Recherche Médicale*) ethical committee and approved by an Institutional Review Board (CPP Ile de France 1).

Behavioral Paradigm and Contrast Sensitivity Function

A psychometric function relating visual detection performance with stimulus contrast levels was calculated using an adaptive estimation of psychometric function parameters (Kontsevich and Tyler 1999) implemented in the Matlab toolbox Palamedes (Kingdom and Prins 2009). This method uses a Bayesian adaptive estimation of the slope and threshold of the psychometric curve and sets on each trial the stimulus contrast that maximizes the expected information to be gained by the participant's response.

Visual stimuli were displayed on a monitor (Hewlett Packard, HP ZR22w, 21.5 inches diagonally measured, and a resolution of 1920 × 1080 pixels) using a computer (Hewlett Packard, HPZ800) and standard stimulus presentation software (Psychophysics Toolbox Version 3, PTB-3) running under Matlab 8.0 (MathWorks, Natick, MA, USA). The screen was positioned at 57 cm from the participant's eyes. Each trial started with a gray resting screen (luminance: 31 cd/m^2) presented for 2000 ms, followed by a central fixation cross (0.5° × 0.5°) displayed along with 2 laterally located rectangular placeholders (6.0° × 5.5°) centered 8.5° to the left and to the right of the screen center, and lasting randomly between 1000 and 1500 ms. Then, the fixation cross became slightly bigger (0.7° × 0.7°, 66 ms) to alert participants of an upcoming event. After an interstimulus interval of 233 ms during which TMS
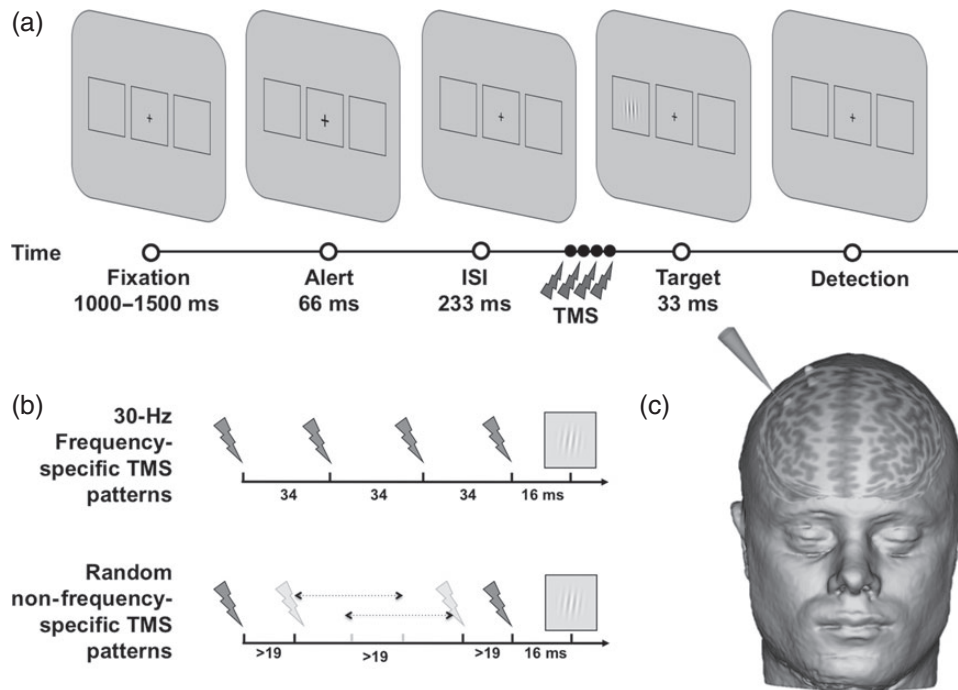
Figure 1. Visual detection paradigm and rhythmic high-beta TMS. (*a*) Sequence of events during a representative trial of the visual paradigm employed in the study to estimate the contrast sensitivity function under either sham or active TMS right frontal patterns. After a variable fixation time, and following the delivery of either sham or active TMS on the right FEF, participants were requested to manually report the localization of a target consisting in a Gabor as having been presented either in the left or the right placeholder. (*b*) Temporal distribution of sham or active TMS for high-beta (30 Hz) *frequency-specific* and *random non-frequency-specific* delivered to the right FEF prior to the Gabor onset. (*c*) TMS coil positioning on the targeted right FEF region in a representative participant.

patterns were delivered (see further details below), a target appeared for 33 ms at the center of 1 of the 2 placeholders (Fig. 1). The target consisted of a Gabor stimulus (3 cycles/degrees spatial frequency, 3.0° ± 0.3° diameter, and minimum and maximum Michelson contrast of 0.005 and 1) with lines oriented vertically. Participants were requested to report the Gabor's location by pressing with their right hand the corresponding button on a computer keyboard ("1" for left and "2" for right). They were required to respond as quickly and as accurately as possible, and forced to provide a response, even when they did not consciously perceive any target during the trial. If the participant did not respond after a 3000-ms response window, the next trial began. Eye movements were monitored across the trial to ensure correct central fixation by means of a high frequency eye-tracker (Eyelink 1000, SR Research, Mississauga, ON, Canada). Fixation was considered broken when participants' gaze was recorded outside a circular spot of 2° radius around the center of the fixation cross, during the 300-ms preceding the target onset and until its offset. In that eventuality, participants received an alert message on the screen and the trial was repeated.

Psychometric contrast sensitivity functions were built using the psi method (Kontsevich and Tyler 1999), an adaptive procedure pursuing both an estimate of the threshold and the slope of the psychometric function relating stimulus contrast with detection performance. In an adaptive procedure, an algorithm considers the prior history of the participant's response to choose the contrast intensity for the next trial. In particular, the psi method selects a contrast level for an upcoming trial by updating a distribution defined across possible threshold and slope values that minimizes the expected entropy, that is, the uncertainty, in the distribution after the completion of the trial. By decreasing the entropy of the distribution, this method increases after each trial the precision of the parameter estimates (Kingdom

and Prins 2009). This method allowed us to estimate both threshold and slope, and thus reconstruct a psychometric function after only 300 trials (Kontsevich and Tyler 1999; Fig. 2). The generating function employed in every experimental condition was a Gumbel (log-Weibull) function with fixed values of a lapse rate of 2% and a guess rate of 50%, according to a two-alternative forced-choice task. The contrast threshold for this function with these parameters is estimated at 80.34% performance. Using the above reported procedures, two independent psychometric functions (one for real and another for sham TMS trials, see further details below) were compiled in parallel during the same testing block. Participants performed a total of 300 trials for each of the two psychometric curves and were allowed to take a short break every 75 trials to minimize fatigue effects.

Transcranial Magnetic Stimulation Procedures

TMS pulses were delivered by means of a biphasic repetitive stimulator using a 70-mm diameter figure-of-eight coil (Magstim SuperRapid 2, The Magstim Company Limited, Whitland, UK). The right FEF region was localized on each individual magnetic resonance imaging (MRI) using Talairach coordinates $x = 31$, $y = -2$, $z = 47$ (Paus 1996), which have been successfully employed in prior experiments to manipulate and improve in humans conscious visual perception (Grosbras and Paus 2002; Chanes et al. 2012, 2013). This region is located within or in the vicinity of the caudal portion of the middle frontal gyrus, immediately rostral to the crossing of the precentral sulcus and the superior frontal sulcus [see Vernet et al. (2014) for a discussion of FEF localization issues]. The structural T_1-weighted MRI scan was uploaded into a stereotaxic system and reconstructed in three-dimensional (3D) space for its use in an online TMS neuronavigation system (Brainsight, Rogue Research, Montreal, QC, Canada).
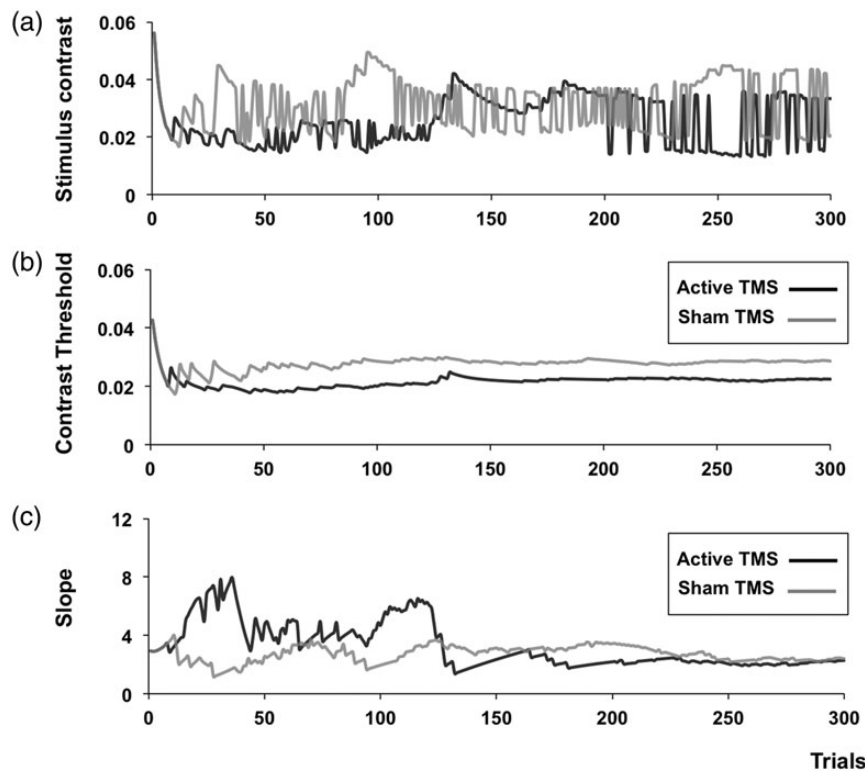
Figure 2. Algorithmical procedure employed to estimate contrast sensitivity functions. (*a*) Stimulus contrast levels presented across an experimental block for either active (black line) or sham (gray line) TMS psychometric functions in a representative participant. Target contrast was chosen on each trial to minimize the uncertainty of the next calculated distribution, defined across possible threshold and slope of the psychometric function. (*b* and *c*) Estimation of the contrast threshold and the function slope throughout the same experimental block leading to the determination of the active and sham TMS psychometric functions, updated after each trial, in the same representative participant.

At all times, the TMS coil was held tangentially to the skull, with its handle oriented approximately 45° in a rostral-to-caudal and lateral-to-medial orientation, that is, approximately parallel to the central sulcus. During the experiment, the position of the active coil was tracked online throughout the experiment and kept steady within an area of <2 mm radius from the targeted site. At the end of the session, for population characterization purposes, the cortical representation of the right primary motor cortex of the *Abductor Pollicis Brevis* muscle was localized, and following standard procedures, the motor threshold at this location was determined as the intensity of single TMS pulses able to induce an activation of this muscle in 50% of the attempts.

TMS procedures followed those which in a prior study by our group had demonstrated improvements in visual detection performance for near-threshold targets (Chanes et al. 2013). TMS patterns consisted in bursts delivered to the FEF prior to target onset. Half of trials included 4-pulse bursts of active TMS, whereas the other half employed equivalent patterns of sham TMS delivered by a second TMS coil placed next to the stimulation site, with the coil's surface perpendicular to the scalp, preventing the magnetic field from reaching the skull and stimulating the brain. The order of active and sham TMS patterns was randomized across trials. The first and last pulses of either sham or active TMS bursts were delivered 118 and 16 ms prior to target onset, respectively. Stimulation intensity was set up 45% of the maximal TMS machine output, which corresponded to 71 ± 12% of their individual motor thresholds.

In this experiment, each participant performed 2 blocks of trials which were counterbalanced in order across subjects (Fig. 1). In the *high-beta frequency-specific block*, we employed either

sham or real bursts of 4 TMS pulses uniformly delivered at 30 Hz across a 102-ms interval (interpulse intervals between 1st–2nd, 2nd–3rd, and 3rd–4th pulses = 34, 34, and 34 ms). Nonetheless, to isolate the effect of the frequency, we compared the latter block with a *random non-frequency-specific* block in which we employed also 102 ms long sham or real 4-pulse bursts with the 2nd and the 3rd pulses randomly shifted in time on a trial-by-trial basis, according to the following constraints: two TMS pulses could not be delivered closer than 19 ms to ensure constant recharge time and pulse intensity by the TMS machine, and the 4 pulses of the burst could not be equally distributed across the burst interval to avoid occurrences of the 30-Hz *rhythmic frequency-specific* patterns tested in the main condition.

Magnetic Resonance Imaging Acquisition

Diffusion MRI scans were obtained on a 3-Tesla MRI scanner (Tim Trio, Siemens Healthcare, Erlangen, Germany) located at the CENIR (Centre de Neuro-Imagerie de Recherche) at the Hôpital de la Pitié Salpêtrière, in Paris, France. Using a 32-channel array coil and a maximum gradient of 28 mT/m, diffusion weighting was isotropically distributed along 60 directions and 6 non-diffusion-weighted volumes were acquired. The first $b0$ image served as an anatomically reference for the correction of participant movements and eddy currents. Imaging parameters were as follows: voxel size $= 1.7 \times 1.7 \times 1.7$ mm^3, repetition time (TR) $= 12\,800$ ms, echo time (TE) $= 88$ ms, $b = 1500$ s/mm^2, and matrix size $= 129 \times 129 \times 71$. Total acquisition time was 14 min and 43 s. A 3D structural T_1-weighted MRI employed to neuronavigate the TMS coil was also recorded from each participant (TR = 2300 ms, TE = 4.18 ms,

matrix size = 256 × 256, and 176 sagittal slices with 1 mm thickness). For technical reasons, diffusion images from one of the participants in the TMS experiment could not be obtained and this participant was not included in the white matter analyses.

Diffusion Data Processing and Estimation of Fiber Orientation

Diffusion images were corrected for head motion and eddy current distortions using affine registration to the first non-diffusion-weighted volume implemented in the FSL software package (FSL 4.1.6—www.fmrib.ox.ac.uk/fsl/). Spatial deformation of the DTI dataset due to susceptibility artifacts was corrected with nonlinear deformation computed from the diffusion images to match the T_1-weighted volume using the Freesurfer Software (Freesurfer 5.0.0, http://surfer.nmr.mgh.harvard.edu/). A spherical deconvolution approach based on the damped version of the Richardson Lucy algorithm as described in Dell'acqua et al. (2010) was employed to estimate fiber orientation distribution (FOD) in each white matter voxel. A first absolute threshold was used to exclude small spurious local maxima due to noise or isotropic voxels and a second relative threshold of 5% of the maximum amplitude of the FOD was applied to remove the remaining local maxima with values greater than the absolute threshold.

Tractography Procedures and Delineation of the Superior Longitudinal Fasciculus

Whole brain tractography was performed starting from every voxel with at least one fiber orientation as a seed. From these voxels and for each fiber orientation, a modified fiber assignment using a continuous tracking algorithm was used to reconstruct streamlines by sequentially piecing together discrete and shortly spaced estimates of fiber orientation forming continuous trajectories. When entering a region with crossing white matter bundles, the algorithm followed the orientation vector of least curvature. Streamlines were halted when a voxel without fiber orientation was reached or when the curvature between two steps exceeded a threshold of 45°. The software used to estimate and reconstruct the orientation vectors and the trajectories from diffusion MRI data was implemented in Matlab 7.11 (MathWorks).

The three branches of the SLF were delineated in both hemispheres following the previously reported procedure [see Supplementary Methods in Thiebaut de Schotten et al. (2011)]. To delineate the SLF I, II, and III, three regions of interest (ROIs) encompassing the white matter of the superior, middle, and inferior/precentral frontal gyri were outlined on a coronal section at the anterior commissure's level. A parietal ROI was also delineated on a coronal section at the level of the posterior commissure. This "and" ROI was common to the three branches of the SLF. The inferior border of frontal and parietal ROIs followed a line between the cingulate sulcus and the circular sulcus and was adjusted individually to encompass each branch of the SLF. A temporal ROI on an axial section was used to exclude streamlines of the arcuate fasciculus, which are not part of the SLF. When required, an ROI outlined on an axial section encompassing the internal and external capsules was employed to eliminate descending fibers. Likewise, a mid-plane ROI encompassing the corpus callosum was used to exclude fibers passing into the opposite hemisphere. All ROIs were drawn manually on a T_1 image coregistered to diffusion images corresponding to each individual participant. Each SLF branch was normalized to the

Montreal Neurological Institute (MNI) mean brain volume using SPM (www.fil.ion.ucl.ac.uk/spm) to create a mean tractography image.

Contrast Sensitivity Data Presentation and White Matter–Visual Performance Correlations

Contrast threshold and slope values obtained from the estimated contrast sensitivity functions (see prior ad hoc method section for details on the Bayesian adaptive procedure employed) were presented in a logarithmic scale and compared between the sham and active TMS conditions. We also calculated performance differences at the contrast threshold level (Fig. 3), and employed this parameter as a measure of relative visual detection *performance modulations*.

A commercially available statistical software package (JMP 10.0.0, SAS, Cary, NC, USA) was used to analyze visual behavioral outcomes and compute the correlations between neurostimulation and tractographic data sets. The volume of the 3 branches of the SLF was determined and divided by the total white matter volume tracked on each participant. The mean *hindrance modulated orientational anisotropy* (HMOA), defined as the absolute amplitude of each lobe of the FOD and considered highly sensitive to axonal myelination, fiber diameter, and axonal density (Dell'Acqua et al. 2013), was individually calculated for each of the three SLF branches.

The Pearson's correlation coefficient between the TMS-induced visual performance modulation (sham TMS minus active TMS effects) at the contrast threshold and the mean HMOA for each branch of the SLF was calculated (JMP 10.0.0, SAS). On the basis that the dorsal attention-orienting network has been shown to be distributed bilaterally in both hemispheres, and considering prior right FEF TMS studies which consistently reported visual modulatory effects for targets in both visual hemifields (Grosbras and Paus 2002, 2003; Chanes et al. 2012, 2013), we also decided to correlate the modulation of behavioral visual outcomes with the HMOA of the three left SLF branches. A post hoc Bonferroni correction was used to compensate for the family-wise error rate in multiple comparisons (uncorrected *$P < 0.05$; corrected **$P < 0.05/12 = 0.004$). The Kolmogorov–Smirnov test was also employed to verify the Gaussian distribution of these variables. Correlation coefficients between HMOA in each SLF branch and the visual modulations induced by *frequency-specific* or *random non-frequency-specific* patterns were compared using the method reported in Steiger (1980). To provide additional support of the robustness of our statistically significant correlations between visual performance outcomes and the HMOA of the SLF I branch, a permutation test based on Pearson's correlation coefficient with 5000 random permutations was also implemented (Groppe et al. 2011). To this end, the mean HMOA of the SLF I in each hemisphere was permuted across our group of participants and the correlation with visual detection gains recalculated for each new version of the modified dataset. The null hypothesis of the permutation test is that the correlation obtained with the initial order is as likely as the correlation obtained with the random permutations of the data.

Results

Impact of High-Beta Frequency-Specific Frontal Patterns on the Contrast Sensitivity Function

We compared the contrast threshold and the slope extracted from the estimated contrast sensitivity function under the
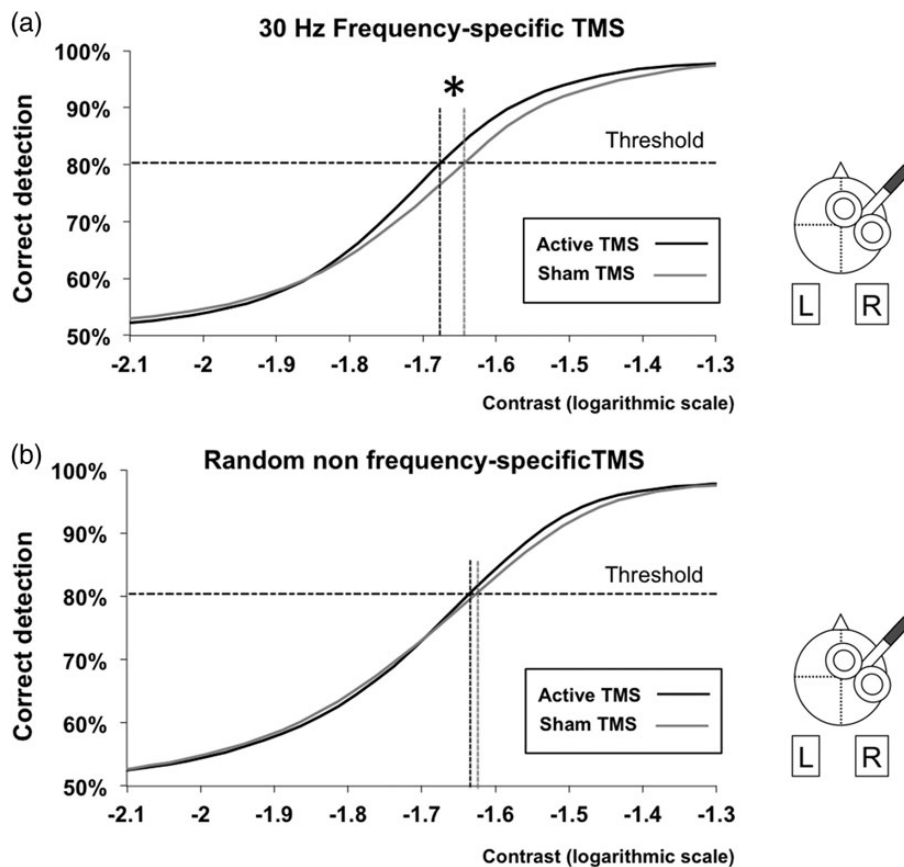
Figure 3. Estimated contrast sensitivity function with high-beta frequency-specific and random non-frequency-specific FEF patterns. Mean contrast sensitivity psychometric function from our cohort of participants under the effects of active (black line) and sham (gray line) TMS consisting in: (*a*) 4-pulse 30 Hz *frequency-specific* patterns or (*b*) *random non-frequency-specific* 4-pulse patterns with an identical duration as the former. Contrast values are presented in a logarithmic scale. Performance levels are presented as the percentage of correct detection. The horizontal dotted line represents the performance threshold (80.3% correct detections). Notice the significant leftward shift in contrast thresholds for active 30 Hz *frequency-specific* patterns when compared with sham (*$P < 0.05$), which was not present when *random non-frequency-specific* 4-pulse patterns were employed.

impact of either active or sham high-beta *frequency-specific* right FEF patterns and their *random non-frequency-specific* counterparts. A 2 × 2 repeated-measure ANOVA with TMS (active or sham) and pattern (*frequency-specific* or *random non-frequency-specific*) revealed a main effect of TMS for the contrast threshold ($t = 8.75$, $P = 0.011$). No other main effect or interaction reached statistical significance ($P > 0.05$). However, based on prior results showing visual improvements under identical right frontal *frequency-specific patterns* for near-threshold targets (Chanes et al. 2013), we analyzed separately the outcomes of the two patterns. Interestingly, the contrast threshold was significantly lower for active than sham *frequency-specific* patterns (paired *t*-test, $t = -2.52$, $P = 0.025$), whereas no differences were found for the *random non-frequency-specific* (paired *t*-test, $t = -1.099$, $P = 0.29$) condition. In contrast, the 2 × 2 repeated-measure ANOVA on the slope revealed no significant main effect or interaction ($P > 0.05$). Analyzed separately, TMS induced no significant effect on the slope of the estimated function for either patterns (*frequency-specific*: paired *t*-test, $t = 0.95$, $P = 0.36$; *random non-frequency-specific*: paired *t*-test, $t = 1.06$, $P = 0.31$; Fig. 3).

Our rhythmic TMS behavioral data support prior evidence on the ability of high-beta rhythmic oscillatory in the right FEF to improve visual sensitivity (Chanes et al. 2013). As an important novelty, it extends such results beyond near-threshold contrast levels, demonstrating their ability to induce a leftward shift of the contrast sensitivity function without modifying its slope,

hence driving a global enhancement of visual performance properties corresponding to a contrast gain mechanism.

White Matter Tractography Analyses and Correlations

To confirm previous findings about hemispheric lateralization and validate our tracking method, we started our analyses by comparing the normalized volume between the three SLF branches of the right and left hemisphere. In agreement with prior reports (Thiebaut de Schotten et al. 2011; Quentin et al. 2015), a branch-specific right hemispheric lateralization pattern involving the SLF III ($t = -3.641$, $P = 0.003$), but neither the SLF I nor the SLF II ($t < 1$), was found once more. We then calculated for each individual participant the visual performance modulation (active TMS–sham TMS) at the contrast threshold level estimated in the sham condition for the high-beta *frequency-specific condition* (Fig. 4). A Kolmogorov–Smirnov test confirmed that this variable and also the HMOA index had a Gaussian distribution. Visual performance modulations induced by high-beta right FEF TMS patterns correlated significantly with the mean HMOA index of the right SLF I branch ($r = -0.78$, $P = 0.0017$), but not with that of any of the remaining right or left SLF branches (rSLF II: $r = -0.20$, $P = 0.51$; rSLF III : $r = -0.39$, $P = 0.19$; lSLF I: $r = -0.17$, $P = 0.58$; lSLF II: $r = 0.45$, $P = 0.12$; lSLF III: $r = -0.06$, $P = 0.83$; Fig. 5).

An ad hoc permutation test confirmed the robustness of the correlation ($P = 0.0012$). Moreover, correlation between individual
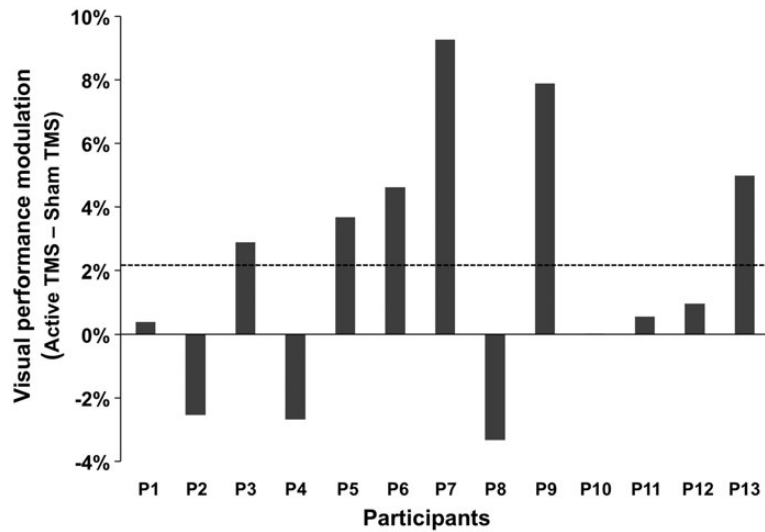
Figure 4. Individual levels of visual detection modulations induced by high-beta frontal frequency-specific patterns. Data are presented as the visual detection modulations (in % change) for study participants included in the white matter analyses. This parameter was calculated by subtracting correct detection performance under the impact of active versus sham stimulation at the threshold contrast level estimated in the sham condition. The horizontal dotted gray line signals the group average for visual performance gains. Notice the large degree of interindividual variability in these outcome measures under the 30-Hz *frequency-specific* right frontal activity patterns, with 6 participants showing large performance increases, 3 participants displaying moderate-to-null visual facilitatory effects, and 3 participants experiencing performance decreases.
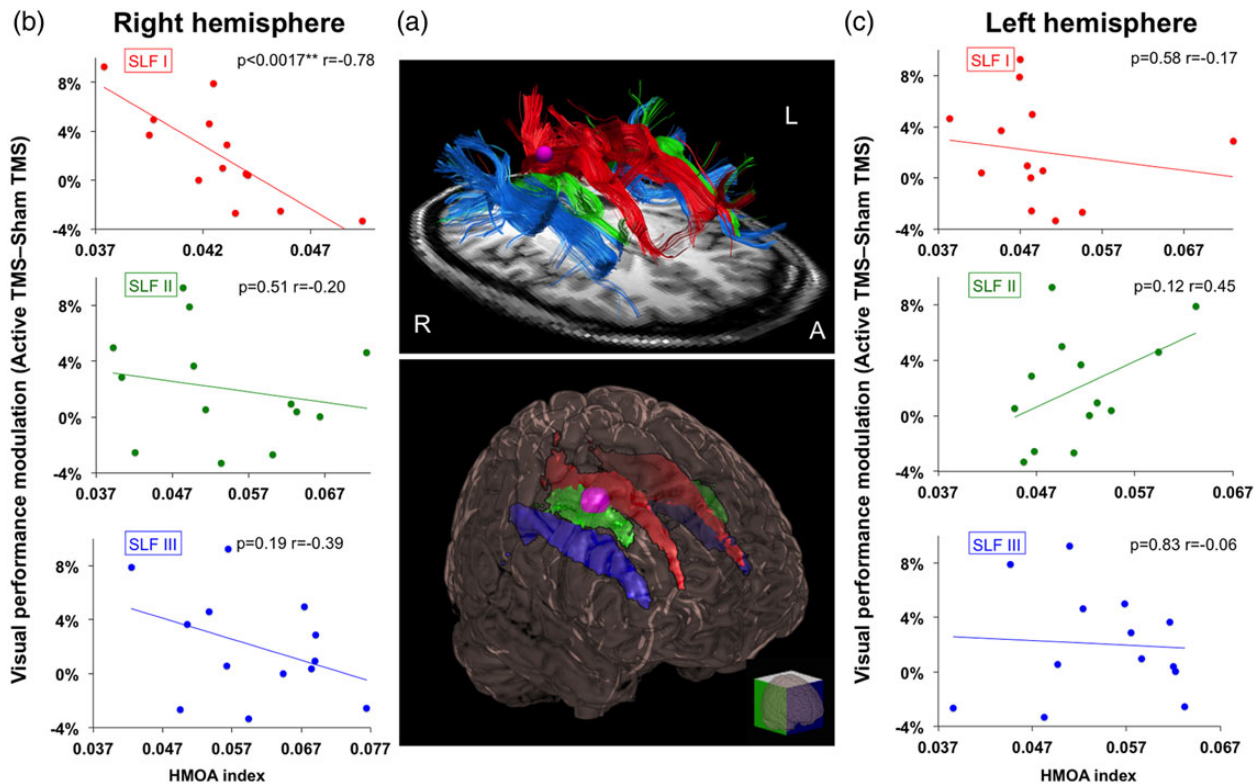

Figure 5. Correlations between white matter diffusion imaging data and visual detection gains associated with frequency-specific right frontal activity. (*a*) Upper panel: Tractographic rendering of the three branches of the SLF in both hemispheres (SLF I in red, SLF II in green, and SLF III in blue) in a representative participant: Lower panel: Glass brain representing on a 3D MNI template the mean SLF I, II, and III in both hemispheres for the whole group of participants (SLF I in red, SLF II in green, and SLF III in blue). Only white matter voxels, which were common to at least 50% of the participants, are shown in the image as part of the tracts. The purple region signals the site of the targeted right FEF area. (*b* and *c*) Correlation plots of the percentage of visual detection gains at threshold contrast level (active TMS–sham TMS) and the mean anisotropy index (or HMOA index) of the three SLF branches in the right and left hemispheres. Notice that only the right SLF I ($r = -0.78$; $P < 0.005$ Bonferroni corrected) branch linking the FEF to the IPS regions showed a significant correlation between the HMOA index and visual detection gains. The asterisks indicate either (*) uncorrected ($P < 0.05$) threshold significance levels or (**) Bonferroni corrected threshold significance levels ($P < 0.05/12$).

visual performance gains (sham TMS–active TMS) induced by the *random non-frequency-specific* patterns and the HMOA index of each SLF branch was also tested and proved non-statistically significant (all $P > 0.10$). To further corroborate that the correlation in the *frequency-specific* condition was specifically related to stimulation frequency, we also confirmed that the correlation coefficient between the SLF I's *HMOA* index and the visual performance gains induced by the *frequency-specific* TMS pattern was significantly higher than the one produced by *random non-frequency-specific* patterns ($P = 0.01$).

Discussion

The results of the current study indicate that frequency-specific right FEF activity at 30 Hz is able to induce a significant decrease in contrast thresholds and a general leftward shift of the contrast sensitivity function, resulting in a global enhancement of visual performance along a large continuum of stimulus contrast levels. Importantly, modulations of contrast thresholds were not accompanied by shifts in the slope of the psychometric function, suggesting that visual ameliorations were driven by a contrast gain mechanism. To the best of our knowledge, this is the first report showing a modulation of contrast sensitivity causally associated with the manipulation of right frontal rhythmic activity, not restricted to near-threshold contrast levels, but spanning to a full spectrum of contrast values.

The rhythmic stimulation pattern employed to manipulate frontal activity was inspired from a non-human primate study (Buschman and Miller 2007), showing correlationally the engagement of 22–34 Hz oscillatory activity along a right fronto-parietal system during a visual search task involving the allocation of endogenous attention. Interestingly, the causal modulation of the contrast sensitivity function reported here matches the effects induced by the engagement of endogenous attention by means of predictive visuo-spatial cues (Ling and Carrasco 2006). This similarity cannot be taken as a direct demonstration, but put together with the fact that our visual amelioration effects were induced in a well known frontal node of the dorsal attentional network, it strengthens the hypothesis that those could have been mediated by the engagement of top down attentional orienting mechanisms operating in the right dorsal fronto-parietal system linking the FEF and the IPS (Corbetta and Shulman 2002; Corbetta et al. 2008; Chica et al. 2011). Moreover, the general leftward shift of the psychometric function consisting in reductions of the contrast threshold, without significant differences on its slope, suggests that visual facilitatory effects were independent of stimulus intensity. In other words, the visual performance consequences of an engagement of right frontal high-beta rhythmic activity are similar to those that could have been achieved by increasing stimulus contrast, whereas a multiplicative response gain, which is not compatible with the outcomes of our study, would have necessarily implied changes in the slope of the psychometric function. All in all, these observations provide support in favor of the contrast gain hypothesis as the underlying mechanism for the visual performance improvements (Reynolds and Desimone 1999; Carrasco et al. 2004) induced causally by right frontal high-beta oscillatory activity.

In a prior study (Chanes et al. 2013), we studied the impact of the same frequency-specific high-beta frontal patterns and demonstrated bilateral improvements of conscious visual detection performance for near-contrast threshold targets. Our current study has been able to reproduce this same outcome employing a two-alternative forced-choice visual detection task, not integrating an explicit and conscious report of target absence or

presence. This result suggests that the contribution of the right FEF to visual perception can operate through long-range frontal connections on early visual areas, and not necessarily by acting on higher level frontal computations leading to visual conscious access. This possibility is coherent with studies showing attentional modulations in striate and extrastriate visual cortices (Reynolds and Desimone 1999; Reynolds et al. 2000; Hol and Treue 2001; Saenz et al. 2002) and also with reports suggesting a direct impact of FEF stimulation on the activity of primary visual areas in non-human primates (Reynolds and Chelazzi 2004; Ekstrom et al. 2009) and humans (Ruff et al. 2006).

In spite of the statistical significance of our intervention which was present only when active frequency-specific TMS patterns were employed, the mean performance modulation at the threshold level, which was around 2.6%, appeared below the magnitude achieved by the deployment of covert attention on contrast appearance (Carrasco et al. 2004). An inspection of individual results suggests, however, that the low magnitude of this effect is likely caused by the large interindividual behavioral variability in response to frontal stimulation, which has been recently associated with interindividual differences in white matter pathways linking the stimulated region and other cortical or subcortical sites of a specific network (Quentin et al. 2013, 2015). Computer simulations (Tononi et al. 1994; Pajevic et al. 2014) and electrophysiological experimental approaches (Fernández et al. 2011; Zaehle and Herrmann 2011) have related white matter pathways to their ability to provide an adequate anatomical basis for interregional synchrony at specific frequency ranges. These hypotheses received further back up from observations suggesting a direct impact of white matter tract maturation during adolescence, likely induced by an increase in myelination (Giedd 2004) subtending a progressive shift toward faster frequencies of oscillatory activity across this same postnatal developmental period (Gasser et al. 1988; Segalowitz et al. 2010). Interestingly, we found that the causal contribution of right frontal high-beta rhythmic activity to visual detection significantly co-varied with interindividual differences of the mean anisotropy index (HMOA) calculated for the first branch of the SLF. This subset of SLF fibers is known to link the right FEF and the right IPS (Thiebaut de Schotten et al. 2011), two sites involved in endogenous attentional orienting (Corbetta and Shulman 2002; Corbetta et al. 2008; Chica et al. 2011). Similarly, the significant correlation between rhythmic TMS modulations and white matter pathway could reflect the ability of a particular network to synchronize these two sites at an exact high-beta frequency according to its specific connectivity (Zaehle et al. 2010).

At difference with our prior report (Quentin et al. 2015) in which we correlated TMS behavioral outcomes and white matter tract volume, we here employed the HMOA index, defined as the absolute amplitude of the fiber orientation distribution in each lobe. This parameter reflects better the microstructural properties specific to a single fiber population and has demonstrated a high sensitivity to fiber tract myelination level, axonal diameter, and axonal density (Dell'Acqua et al. 2013). These first two physiological parameters are known to impact conduction time. Following the fronto-parietal synchronization hypothesis, the action potential elicited by the first of the four pulses uniformly delivered to the right FEF would need to reach a parietal postsynaptic region at a particular timing, coherent with the delivery of the following pulse (33 ms thereafter for 30 Hz stimulation). Across-subject differences in white matter myelination do impact conduction velocity and either slightly accelerate or delay conduction time by a few milliseconds, precluding an efficient synchronization of the network at a very specific frequency

and leading to lower levels of visual improvement or no visual enhancement at all. In this framework, the correlation we present here supports a crucial role for fronto-parietal pathways in their ability to synchronize frontal and parietal areas, at frequency bands similar to those previously identified in correlational studies with electrophysiological recordings (Buschman and Miller 2007; Phillips and Takeda 2009).

Finally, and not less interestingly, despite differences (Quentin et al. 2013) and similarities (Quentin et al. 2015) in the stimulation patterns employed on each case, the current outcome provides additional experimental support in favor of an inverse association between TMS-modulated behaviors and white matter connectivity. As mentioned in prior publications, this result might seem counterintuitive, as larger tract volumes or higher probability of connection have been often associated with more effective connectivity and information transfer (Glasser and Rilling 2008; Thiebaut de Schotten et al. 2011). Alternatively, however, less anisotropic pathways could prove more efficient in conveying neural signals, particularly when those are artificially induced by not always sufficiently focal noninvasive neurostimulation sources (Quentin et al. 2013, 2015).

In summary, our study provides novel and converging evidence that pre-target onset patterns of high-beta rhythmic activity on the right FEF play a major role in top-down visual modulation. We also gathered additional support for the notion that this modulation is strongly dependent on the microstructure of the right SLF I, suggesting an association between these pathway and the ability to convey rhythmic signal between frontal and parietal regions.

Authors' Contributions

A.V.-C. developed the main concept of this project, provided the funding, and was in charge of its supervision. R.Q., S.E.F., and A.V.-C. developed the specific hypotheses and ideas and co-designed the study. R.Q., M.V., A.V.-C., and M.T. performed the TMS experiments. R.Q. analyzed the behavioral data, the diffusion data, and computed the correlations. R.Q., A.V.-C., and M.V. interpreted the data. R.Q. and A.V.-C. prepared the final figures and wrote the draft of the manuscript, and M.V., L.C., and P.B. read and provided suggestions to the final version of the manuscript.

Funding

Notes

References

Buschman TJ, Miller EK. 2007. Top-down versus bottom-up control of attention in the prefrontal and posterior parietal cortices. Science. 315(5820):1860–1862.

Buzsáki G, Draguhn A. 2004. Neuronal oscillations in cortical networks. Science. 304(5679):1926–1929.

Cannon J, McCarthy MM, Lee S, Lee J, Börgers C, Whittington MA, Kopell N. 2014. Neurosystems: brain rhythms and cognitive processing. Eur J Neurosci. 39(5):705–719.

Carrasco M, Ling S, Read S. 2004. Attention alters appearance. Nat Neurosci. 7(3):308–313.

Chanes L, Chica AB, Quentin R, Valero-Cabré A. 2012. Manipulation of pre-target activity on the right frontal eye field enhances conscious visual perception in humans. PLoS ONE. 7 (5):e36232.

Chanes L, Quentin R, Tallon-Baudry C, Valero-Cabré A. 2013. Causal frequency-specific contributions of frontal spatiotemporal patterns induced by noninvasive neurostimulation to human visual performance. J Neurosci. 33(11):5000–5005.

Chica AB, Bartolomeo P, Valero-Cabré A. 2011. Dorsal and ventral parietal contributions to spatial orienting in the human brain. J Neurosci. 31(22):8143–8149.

Corbetta M, Patel G, Shulman GL. 2008. The reorienting system of the human brain: from environment to theory of mind. Neuron. 58(3):306–324.

Corbetta M, Shulman GL. 2002. Control of goal-directed and stimulus-driven attention in the brain. Nat Rev Neurosci. 3 (3):201–215.

Dell'acqua F, Scifo P, Rizzo G, Catani M, Simmons A, Scotti G, Fazio F. 2010. A modified damped Richardson-Lucy algorithm to reduce isotropic background effects in spherical deconvolution. NeuroImage. 49(2):1446–1458.

Dell'Acqua F, Simmons A, Williams SCR, Catani M. 2013. Can spherical deconvolution provide more information than fiber orientations? Hindrance modulated orientational anisotropy, a true-tract specific index to characterize white matter diffusion. Hum Brain Mapp. 34(10):2464–2483.

Ekstrom LB, Roelfsema PR, Arsenault JT, Kolster H, Vanduffel W. 2009. Modulation of the contrast response function by electrical microstimulation of the macaque frontal eye field. J Neurosci. 29(34):10683–10694.

Ergenoglu T, Demiralp T, Bayraktaroglu Z, Ergen M, Beydagi H, Uresin Y. 2004. Alpha rhythm of the EEG modulates visual detection performance in humans. Brain Res Cogn Brain Res. 20(3):376–383.

Fernández A, Ríos-Lago M, Abásolo D, Hornero R, Álvarez-Linera J, Paul N, Maestù F, Ortiz T. 2011. The correlation between white-matter microstructure and the complexity of spontaneous brain activity: a diffusion tensor imaging-MEG study. NeuroImage. 57(4):1300–1307.

Foxe JJ, Simpson GV, Ahlfors SP. 1998. Parieto-occipital approximately 10 Hz activity reflects anticipatory state of visual attention mechanisms. Neuroreport. 9(17):3929–3933.

Fries P. 2005. A mechanism for cognitive dynamics: neuronal communication through neuronal coherence. Trends Cogn Sci. 9(10):474–480.

Fuggetta G, Fiaschi A, Manganotti P. 2005. Modulation of cortical oscillatory activities induced by varying single-pulse

transcranial magnetic stimulation intensity over the left primary motor area: a combined EEG and TMS study. NeuroImage. 27(4):896–908.

Gasser T, Jennen-Steinmetz C, Sroka L, Verleger R, Möcks J. 1988. Development of the EEG of school-age children and adolescents. II. Topography. Electroencephalogr Clin Neurophysiol. 69(2):100–109.

Giedd JN. 2004. Structural magnetic resonance imaging of the adolescent brain. Ann N Y Acad Sci. 1021:77–85.

Glasser MF, Rilling JK. 2008. DTI tractography of the human brain's language pathways. Cereb Cortex. 18(11):2471–2482.

Gould IC, Rushworth MF, Nobre AC. 2011. Indexing the graded allocation of visuospatial attention using anticipatory alpha oscillations. J Neurophysiol. 105(3):1318–1326.

Groppe DM, Urbach TP, Kutas M. 2011. Mass univariate analysis of event-related brain potentials/fields I: a critical tutorial review. Psychophysiology. 48(12):1711–1725.

Grosbras MH, Paus T. 2002. Transcranial magnetic stimulation of the human frontal eye field: effects on visual perception and attention. J Cogn Neurosci. 14(7):1109–1120.

Grosbras MH, Paus T. 2003. Transcranial magnetic stimulation of the human frontal eye field facilitates visual awareness. Eur J Neurosci. 18(11):3121–3126.

Hol K, Treue S. 2001. Different populations of neurons contribute to the detection and discrimination of visual motion. Vision Res. 41(6):685–689.

Kingdom FAA, Prins N. 2009. Psychophysics: A Practical Introduction (Édition: Har/Psc.). London: Academic Press.

Kontsevich LL, Tyler CW. 1999. Bayesian adaptive estimation of psychometric slope and threshold. Vision Res. 39(16):2729–2737.

Ling S, Carrasco M. 2006. Sustained and transient covert attention enhance the signal via different contrast response functions. Vision Res. 46(8–9):1210–1220.

Pajevic S, Basser PJ, Fields RD. 2014. Role of myelin plasticity in oscillations and synchrony of neuronal activity. Neuroscience. 276:135–147.

Paus T. 1996. Location and function of the human frontal eye-field: a selective review. Neuropsychologia. 34(6):475–483.

Pestilli F, Ling S, Carrasco M. 2009. A population-coding model of attention's influence on contrast response: estimating neural effect from psychophysical data. Vision Res. 49(10):1144–1153.

Pestilli F, Viera G, Carrasco M. 2007. How do attention and adaptation affect contrast sensitivity? J Vis. 7(7):1–12. 9.

Phillips S, Takeda Y. 2009. Greater frontal-parietal synchrony at low gamma-band frequencies for inefficient than efficient visual search in human EEG. Int J Psychophysiol. 73(3):350–354.

Quentin R, Chanes L, Migliaccio R, Valabregue R, Valero-Cabre A. 2013. Fronto-tectal white matter connectivity mediates facilitatory effects of non-invasive neurostimulation on visual detection. NeuroImage. 82:344–354.

Quentin R, Chanes L, Vernet M, Valero-Cabré A. 2015. Fronto-parietal anatomical connections influence the modulation of conscious visual perception by high-beta frontal oscillatory activity. Cereb Cortex. 25(8):2095–2101.

Reynolds JH, Chelazzi L. 2004. Attentional modulation of visual processing. Ann Rev Neurosci. 27(1):611–647.

Reynolds JH, Desimone R. 1999. The role of neural mechanisms of attention in solving the binding problem. Neuron. 24(1):19–29.

Reynolds JH, Pasternak T, Desimone R. 2000. Attention increases sensitivity of V4 neurons. Neuron. 26(3):703–714.

Romei V, Driver J, Schyns PG, Thut G. 2011. Rhythmic TMS over parietal cortex links distinct brain frequencies to global versus local visual processing. Curr Biol. 21(4):334–337.

Romei V, Gross J, Thut G. 2010. On the role of prestimulus alpha rhythms over occipito-parietal areas in visual input regulation: correlation or causation? J Neurosci. 30(25):8692–8697.

Romei V, Thut G, Mok RM, Schyns PG, Driver J. 2012. Causal implication by rhythmic transcranial magnetic stimulation of alpha frequency in feature-based local vs. global attention. Eur J Neurosci. 35(6):968–974.

Rosanova M, Casali A, Bellina V, Resta F, Mariotti M, Massimini M. 2009. Natural frequencies of human corticothalamic circuits. J Neurosci. 29(24):7679–7685.

Ruff CC, Blankenburg F, Bjoertomt O, Bestmann S, Freeman E, Haynes J-D, Rees G, Josephs O, Deichmann R, Driver J. 2006. Concurrent TMS-fMRI and psychophysics reveal frontal influences on human retinotopic visual cortex. Curr Biol. 16(15):1479–1488.

Saenz M, Buracas GT, Boynton GM. 2002. Global effects of feature-based attention in human visual cortex. Nat Neurosci. 5(7):631–632.

Sauseng P, Klimesch W, Heise KF, Gruber WR, Holz E, Karim AA, Glennon M, Gerloff C, Birbaumer N, Hummel FC. 2009. Brain oscillatory substrates of visual short-term memory capacity. Curr Biol. 19(21):1846–1852.

Sauseng P, Klimesch W, Stadler W, Schabus M, Doppelmayr M, Hanslmayr S, Gruber WR, Birbaumer N. 2005. A shift of visual spatial attention is selectively associated with human EEG alpha activity. Eur J Neurosci. 22(11):2917–2926.

Segalowitz SJ, Santesso DL, Jetha MK. 2010. Electrophysiological changes during adolescence: a review. Brain Cogn. 72(1):86–100.

Steiger JH. 1980. Tests for comparing elements of a correlation matrix. Psychol Bull. 87:245–251.

Thiebaut de Schotten M, Dell'Acqua F, Forkel SJ, Simmons A, Vergani F, Murphy DGM, Catani M. 2011. A lateralized brain network for visuospatial attention. Nat Neurosci. 14(10):1245–1246.

Thut G, Nietzel A, Brandt SA, Pascual-Leone A. 2006. Alpha-band electroencephalographic activity over occipital cortex indexes visuospatial attention bias and predicts visual target detection. J Neurosci. 26(37):9494–9502.

Thut G, Veniero D, Romei V, Miniussi C, Schyns P, Gross J. 2011. Rhythmic TMS causes local entrainment of natural oscillatory signatures. Curr Biol. 21(14):1176–1185.

Tononi G, Sporns O, Edelman GM. 1994. A measure for brain complexity: relating functional segregation and integration in the nervous system. Proc Natl Acad Sci USA. 91(11):5033–5037.

Van Der Werf YD, Paus T. 2006. The neural response to transcranial magnetic stimulation of the human motor cortex. I. Intracortical and cortico-cortical contributions. Exp Brain Res. 175(2):231–245.

Vernet M, Quentin R, Chanes L, Mitsumasu A, Valero-Cabré A. 2014. Frontal eye field, where art thou? Anatomy, function, and non-invasive manipulation of frontal regions involved in eye movements and associated cognitive operations. Front Integr Neurosci. 8:66. doi:10.3389/fnint.2014.00066.

Worden MS, Foxe JJ, Wang N, Simpson GV. 2000. Anticipatory biasing of visuospatial attention indexed by retinotopically specific alpha-band electroencephalography increases over occipital cortex. J Neurosci. 20(6):RC63.

Zaehle T, Herrmann CS. 2011. Neural synchrony and white matter variations in the human brain—relation between evoked gamma frequency and corpus callosum morphology. Int J Psychophysiol. 79(1):49–54.

Zaehle T, Rach S, Herrmann CS. 2010. Transcranial alternating current stimulation enhances individual alpha activity in humans EEG. PLoS One. 5(11):e13766.